Understanding the trend in the Curie temperatures of Co_2-based Heusler compounds: *Ab initio* calculations

J. Kübler*
Institut für Festkörperphysik, Technische Universität Darmstadt, D-64289 Darmstadt, Germany

G. H. Fecher and C. Felser
Institut für Anorganische und Analytische Chemie, Johannes Gutenberg-Universität, D-55128 Mainz, Germany
(Received 1 April 2007; revised manuscript received 23 May 2007; published 10 July 2007)

The Curie temperatures for the Heusler compounds Co_2TiAl, Co_2VGa, Co_2VSn, Co_2CrGa, Co_2CrAl, Co_2MnAl, Co_2MnSn, Co_2MnSi, and Co_2FeSi are determined *ab initio* from the electronic structure obtained with the local-density functional approximation and/or the generalized gradient approximation. Frozen spin spirals are used to model the excited states needed to evaluate the spherical approximation for the Curie temperature. The spherical approximation is found to describe the experimental Curie temperatures very well which, for the compounds selected, extend over the range from 95 to 1100 K; as a function of the valence electron count, they show an approximately linear trend which finds an explanation by our calculations.

DOI: 10.1103/PhysRevB.76.024414 PACS number(s): 75.30.−m, 71.20.Be, 61.18.Fs

I. INTRODUCTION

Heusler compounds have been known for more than 100 years.[1] Recently, they had an astonishing comeback because of their high spin polarization and their possible application in the field of spin-electronics and magnetoresistive devices. An important subset of the Heusler compounds attracting special interest are the Co_2-based Heusler compounds with the formula Co_2XY, where X may be Ti, V, Cr, Mn, or Fe and Y may be Al, Ga, Si, or another main group metal.[2–5] The reason is that a large number of these Co_2-based compounds appear to be half-metallic ferromagnets in electronic structure calculations. This means that their minority-spin electrons possess a sizable gap around the Fermi energy, thus resulting in 100% spin polarization.[2,3,6–9] The half-metallicity is advantageous for spintronic devices in terms of achieving high tunnel magnetoresistance (TMR) ratios in tunnel junctions or efficient spin injection from ferromagnetic electrodes into semiconductors. The first significant magnetoresistive effect in Heusler compounds was observed in $Co_2Cr_{0.6}Fe_{0.4}Al$ powder compacts.[6] This alloy exhibits in thin film devices a TMR ratio of 317% at 4 K.[10] Large TMR ratios were recently reported for $Co_2FeAl_{0.5}Si_{0.5}$ with more than 175% at room temperature.[11] A TMR ratio of 570% at 4 K was reported for Co_2MnSi.[12]

The success of the local spin-density functional approximation (LSDA)[13] for the determination of the electronic structure of the ground state of solids need not be emphasized here.[14] Even though some important many-body effects require special attention and corrections to the LSDA are necessary, it is clear that the LSDA together with suitable computer codes provides a very powerful tool to understand ground-state properties.

The determination of the energies of excited states to obtain finite-temperature properties is somewhat more problematic. For magnetic systems, one invokes the adiabatic approximation[15] and freezes noncollinear spin arrangements that are assumed to give the energies necessary for a thermodynamic treatment. For the latter, one may follow Moriya's approach[16] and derive[17] an approximation for the Curie temperature of itinerant-electron magnets within the LSDA or the generalized gradient approximation (GGA).[18] This treatment of thermodynamics is called the spherical approximation[16] and is superior to the well-known mean-field approximation. In Sec. II and the Appendix, we give a brief exposition of our treatment of the thermodynamic problem and list some details concerning the numerical work. In Sec. III, we apply the theory to the compounds Co_2TiAl, Co_2VGa, Co_2VSn, Co_2CrGa, Co_2CrAl, Co_2MnAl, Co_2MnSn, Co_2MnSi, as well as Co_2FeSi. These were selected from a larger set of Co_2-based Heusler compounds in order to study a wide range of Curie temperatures extending from 95 to 1100 K with magnetic moments ranging from 1 μ_B to 6 μ_B per formula unit. After discussing the trend in the Curie temperatures, we summarize our results in Sec. IV.

II. COMPUTATIONAL DETAILS

The theoretical basis for calculating the Curie temperature of an itinerant-electron ferromagnet in the spherical approximation has been described in Ref. 17. Thus, only some salient facts need be collected here.

The LSDA or the GGA is employed to obtain low-lying excited states from the total energies of frozen spin spirals having wave vectors $\mathbf{q}$.[19–21] The total energies are expressed as exchange energies or exchange functions, $j_{\tau\tau'}(\mathbf{q})$, which depend on two basis vectors of the constituent magnetic atoms, τ and τ', and on wave vectors that span the irreducible part of the Brillouin zone (BZ). If the total energy due to a spin spiral is written as $E(\mathbf{q})$, then the exchange functions are defined through $\Delta E(\mathbf{q})=E(\mathbf{q})-E(0)$ with

$$E(\mathbf{q}) = \sum_{\tau\tau'} M_\tau M_{\tau'} [j_{\tau\tau'}(\mathbf{q}) \sin\theta_\tau \sin\theta_{\tau'} \cos(\varphi_\tau - \varphi_{\tau'}) + j_{\tau\tau'}(0) \cos\theta_\tau \cos\theta_{\tau'}], \quad (1)$$

where θ_τ and φ_τ are the polar coordinates for the magnetic moment vector of atom τ possessing the moment M_τ. A

TABLE I. Collection of pertinent experimental and calculated data for nine representative Co_2-based Heusler compounds. The quantity N_V is the number of valence electrons, and the magnetic moments M^{expt} and M^{calc} are given in μ_B per unit cell. The local moment for Co is denoted by $\mathcal{L}_{Co}$ and those of the other magnetic atoms in the cell by $\mathcal{L}_X$, all in units of μ_B. The Curie temperatures T_C^{SP} were calculated by means of Eq. (2), given in K.

Compound	N_V	a (Å)	M^{expt}	M^{calc}	$\mathcal{L}_{Co}$	$\mathcal{L}_X$	T_C^{SP}	T_C^{expt}
Co_2TiAl[a]	25	5.847	0.74	1.00	0.570	−0.139	157	134
Co_2VGa[a]	26	5.779	1.92	2.00	0.914	0.172	368	352
Co_2VSn[a]	27	5.960	1.21	1.80	0.677	0.445	103	95
Co_2CrGa[b]	27	5.805	3.01	3.06	0.575	1.911	362	495
Co_2CrAl[a]	27	5.727	1.55	3.00	0.669	1.661	341	334
Co_2MnAl[a]	28	5.749	4.04	4.05	0.590	2.877	609	697
Co_2MnSi[a]	29	5.645	4.90	5.00	0.669	3.061	990	985
Co_2MnSn[a]	29	5.984	5.08	5.02	0.885	3.254	899	829
Co_2FeSi[c]	30	5.640	6.00	5.38	1.307	2.762	1185	1100

[a]Lattice constant and experimental Curie temperature from Refs. 26–29.
[b]Lattice constants and Curie temperature from Ref. 30.
[c]Lattice constant and Curie temperatures from Refs. 8, 31, and 32.

choice has to be made for the angles θ_τ and φ_τ. Kleinman and co-workers[22,23] showed for ferromagnets, ferrimagnets, and antiferromagnets in the adiabatic approximation that the spin-wave energy is given by the energy increase divided by the reduction of the total spin z component due to the excitation of the spins. This means that small angles of tilt θ_τ give a reliable estimate for the low-energy excitations [see, for instance, Eq. (14) of Ref. 22]. It is not clear whether higher spin-wave branches are obtained accurately.[23] The choice of the angles φ_τ is made such that the exchange functions can be extracted from Eq. (1) as shown in the Appendix.

The total energy is computed using the force theorem,[24,25] i.e., the band energies are summed up to the Fermi energy for a given spin configuration using for these calculations the self-consistent ground-state potential.

The numerical work done in this paper was done with the augmented-spherical-wave (ASW) method,[33] where the atomic sphere approximation is used for the construction of the effective crystal potential and the von Barth–Hedin[34] approximation for exchange and correlation. The GGA calculations were carried out with the full-potential method derived from the ASW method by Knöpfle *et al.*,[35] which employs the GGA potentials of Perdew *et al.*[18] The crystal structure used was $L2_1$ with the experimental lattice constants listed in Table I.

The spherical approximation (sometimes also called random phase approximation) for obtaining an estimate of the Curie temperature is valid for itinerant-electron magnets covering the whole range from weak ferromagnetism to the local-moment (Heisenberg) limit.[16] The Curie temperature in this approximation is given by

$$k_B T_c^{SP} = \frac{2}{3} \sum_\tau \mathcal{L}_\tau^2 \left[\frac{1}{N} \sum_{\mathbf{q}n} \frac{1}{j_n(\mathbf{q})} \right]^{-1}. \quad (2)$$

Here, the three exchange functions $j_n(\mathbf{q})$ are eigenvalues of a secular equation and are given in the Appendix in terms of the four quantities sufficient for the description of the magnetism of Heusler compounds, Co_2XY: $j_{11}(\mathbf{q})$ describes the exchange interaction between the magnetic X atoms, $j_{22}(\mathbf{q})$ between the Co atoms having the same basis vectors, $j_{12}(\mathbf{q})$ between the Co and X atoms, and $j_{23}(\mathbf{q})$ between the Co atoms with different basis vectors. They are extracted from Eq. (1) by means of the algorithm described in the Appendix. The quantity $\mathcal{L}_\tau$ in Eq. (2) describes the local moment of the atom at site τ. In principle, it must be determined self-consistently [see Eq. (12) in Ref. 17], but an acceptable approximation for Heusler compounds is $\mathcal{L}_\tau = M_\tau$, where M_τ is the zero temperature moment of the atom at site τ. This is so because Heusler compounds possess rather localized moments.[2]

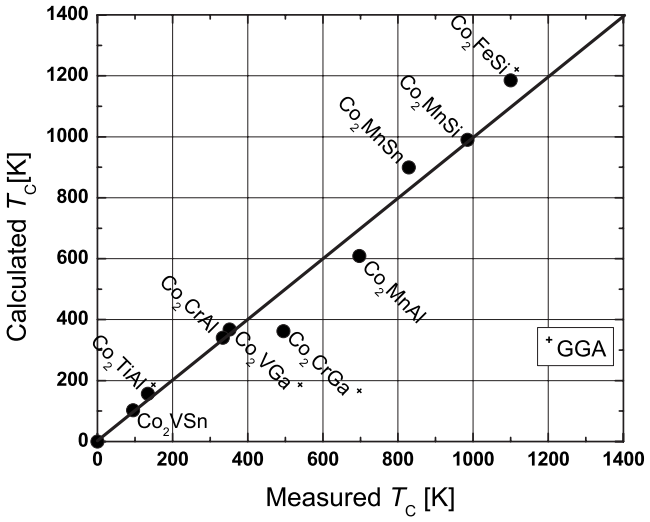

FIG. 1. Calculated versus measured Curie temperatures.

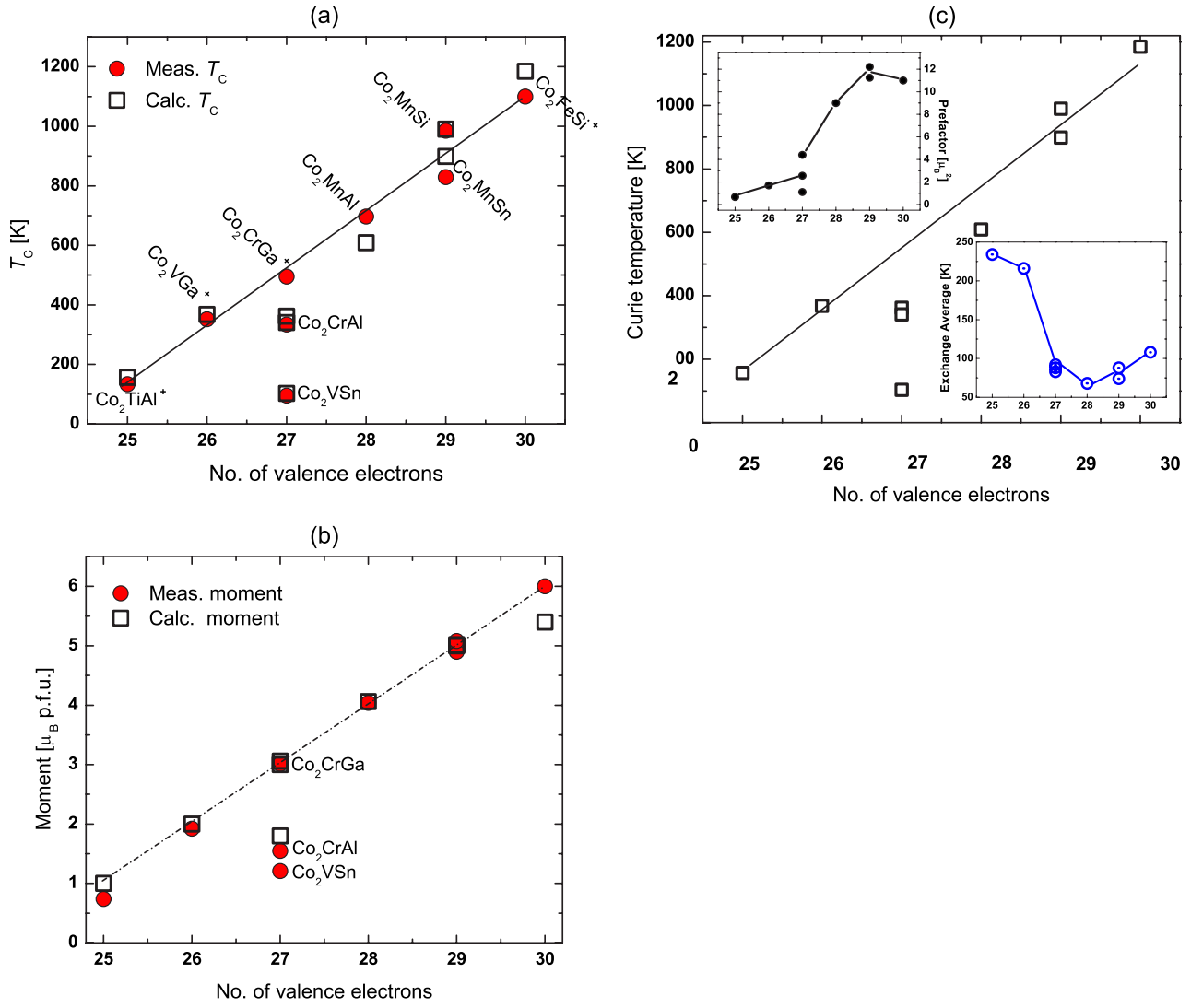

FIG. 2. (Color online) (a) Calculated (squares) and measured (circles) Curie temperatures versus the number of valence electrons. (b) Calculated (squares) and measured (circles) magnetic moments versus the number of valence electrons. (c) Calculated Curie temperatures (squares) versus the number of valence electrons. The insets give the computed values of the two parts of Eq. (2), the prefactor and the exchange average.

III. RESULTS AND DISCUSSION

We begin by showing the calculated Curie temperatures plotted versus the measured values in Fig. 1. This figure is a strong indication that the spherical approximation applied here is useful and supplies, with only few exceptions, rather precise estimates. As indicated in the figure, the GGA was used for the compounds Co_2TiAl, Co_2VGa, Co_2CrGa, and Co_2FeSi; in all other cases, the LSDA gave more satisfactory results. It should be noted that the need to apply the GGA arises for the border cases of low and high numbers of valence electrons, N_V (see Table I which contains all pertinent data for the Co_2-based Heusler compounds).

It has been recognized earlier[4,8,31,32] that the Curie temperatures of the Co_2-based Heusler compounds follow an approximately linear trend when viewed as a function of the magnetic moments. With only few exceptions, this establishes also an approximately linear trend as a function of the number of valence electrons, N_V, since the magnetic moments of these Heusler compounds follow the Slater-Pauling curve.[3,14] This connection is shown in Fig. 2(a), where the calculated and the measured Curie temperatures are displayed as a function of N_V, and in Fig. 2(b), where a section of the Slater-Pauling curve is shown, using both measured and experimental values for the magnetic moments per unit cell.

All straight lines in Fig. 2 are meant to guide the eye; the linear trends in Figs. 2(a) and 2(b) are clearly visible and well understood in the Slater-Pauling case [Fig. 2(b)]; the exceptions for N_V=27 as well as the borderline cases will be discussed below.

The linear trend in the Curie temperatures is obviously broken if the number of valence electrons is N_V=27. An explanation by means of Fig. 2(c) is as follows.

We assume that Eq. (2) is a good starting point. A glance at this equation reveals that two rather simple mechanisms

need be discussed to understand the desired trend, one is contained in the prefactor $\Sigma_\tau \mathcal{L}_\tau^2$, the other in the exchange average $[(1/N)\Sigma_{\mathbf{q}n} 1/j_n(\mathbf{q})]^{-1}$. Computed values for the prefactor are easily obtained with the data given in Table I and are shown in the upper left-hand inset of Fig. 2(c); the calculated exchange average is given in the lower right-hand inset obtained by setting the prefactor in Eq. (2) equal to 1. Multiplying these two quantities, we obtain the calculated Curie temperatures shown as squares in Fig. 2(c). Clearly seen is the changeover of two trends at N_V=27. Quite remarkably, the exchange average is largest for N_V=25, decreasing for increasing N_V to as low a value as 66 K for Co_2MnAl at N_V=28. By virtue of the low value of the prefactor, the calculated Curie temperature of Co_2VSn is only 103 K, in contrast to Co_2CrGa and Co_2CrAl for which the calculated local moment of Cr is nearly $2\mu_B$ (see Table I), resulting in values of the Curie temperature larger than 300 K. The changeover is also supported by experimental observations. The largest deviation from the linear trend of the Curie temperatures and from the Slater-Pauling behavior is observed for 27 valence electron compounds.[4,32] Co_2CrAl together with $Co_2Cr_{0.6}Fe_{0.4}Al$ (Ref. 6) are among the best investigated Heusler compounds. The instability of Co_2CrAl moment is related to B2-like disorder and an antiferromagnetic coupling of Cr with its neighbors, leading to ferrimagnetic behavior[36] which is not obtained by the calculations in the $L2_1$ structure (see Table I). In spite of this, the Curie temperature is estimated within 2% of the experimental value. This could be taken to mean that the disorder-produced low moment has no large influence on the long-range order.

There are two more cases in Table I where the computed moments are noticeably lower than the experimental ones but the estimated Curie temperatures are within 17% and 8% of the measured values; these are, respectively, Co_2TiAl and Co_2VSn. We speculate that this may have an explanation similar to the case of Co_2CrAl.

The larger picture one sees in Fig. 2(c) is the induced magnetism of Ti and V for N_V=25–27. Overlapping at N_V=27 is the pronounced magnetism of Cr. For larger numbers of valence electrons, the magnetism of Mn and Fe dominates that of Co. The exchange average increases but reaches only 108 K at N_V=30, the upward trend in the Curie temperatures being due to the large local moments that boost the exchange average.

We will show now that the electronic structure of the Heusler compounds reveals the reason for the trend in the exchange average. A selected set of spin-resolved density-of-states (DOS) curves is given in Figs. 3–5 where the Fermi energy is at the origin and the majority-spin states (up-spin) are at the upper halves, the lower halves giving the minority-spin states (down-spin) and show the gap which is typical for the Co_2-based Heusler compounds.

In an itinerant-electron ferromagnet like those considered here, the up- and down-spin electrons move independently at T=0.[14] At finite temperatures, the nature of the states and thus the fate of the gap are discussed controversially and still under investigation,[37] but it is clear that noncollinear states as those used here to obtain the exchange functions will hybridize, leading to states of both spin directions in the gap.

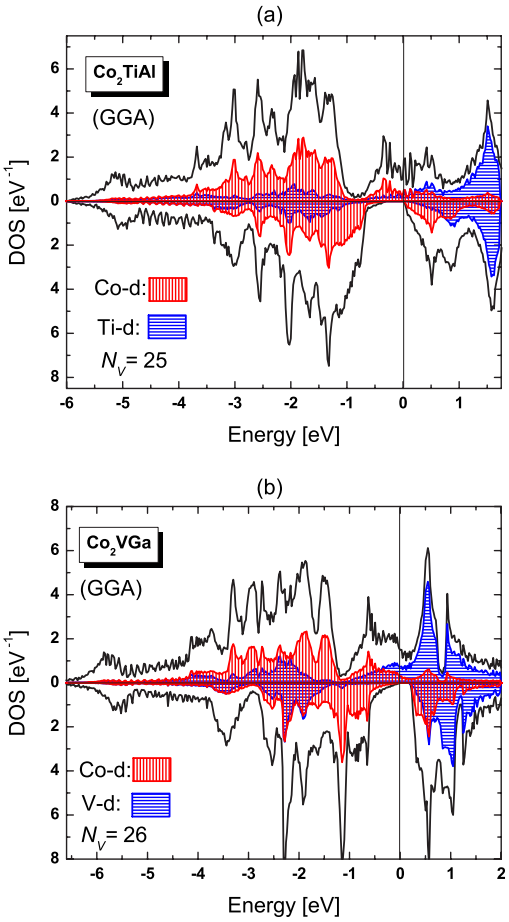

FIG. 3. (Color online) Spin-resolved density of states (DOS) of (a) Co_2TiAl where the number of valence electrons is N_V=25 and (b) Co_2VGa with N_V=26.

Figures 3(a) and 3(b) each show a large gap in the down-spin states at and just below the Fermi energy. Keeping in mind that the total-energy differences which give the exchange functions for each value $\mathbf{q}$ are obtained from integrals over the DOS up to the Fermi energy E_F, one understands qualitatively that the largest changes are sampled when the integral extends over all or most of the gap as is the case in Figs. 3(a) and 3(b).

The large values of the exchange averages shown in Fig. 2(c) for N_V=25 and 26 are thus most likely due to the gap below E_F where hybridization adds spin-down states to Eq. (1). The two density-of-states curves shown in Fig. 4 for N_V=27 support this picture. The low value of the exchange average for N_V=28 finds an explanation in Fig. 5(a) where the fully spin-polarized states are above E_F and thus not available for the total-energy differences. The increase of the exchange average for N_V=29 and N_V=30 finds the same explanation in Figs. 5(b) and 5(c), albeit on a different scale because the density of states at and near E_F is smaller.

The closing remark brings us to Co_2FeSi for which the calculated magnetic moment in Table I is smaller than the measured one, in contrast to the other cases studied here. According to Refs. 8, 31, and 32, the total magnetic moment is $6\mu_B$ and the compound is half-metallic. Both the LSDA and the GGA do not succeed in describing this state cor-

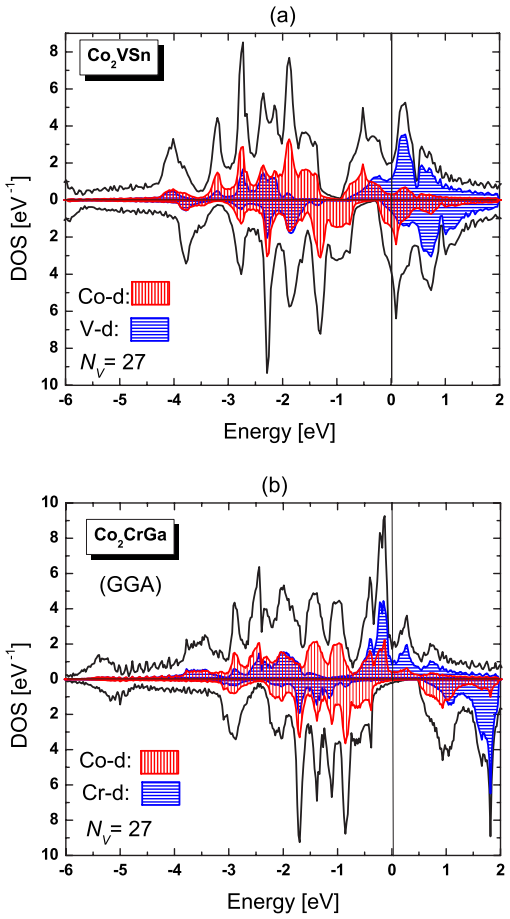

FIG. 4. (Color online) Spin-resolved density of states (DOS) of (a) Co_2VSn and (b) Co_2CrGa. The number of valence electrons is 27.

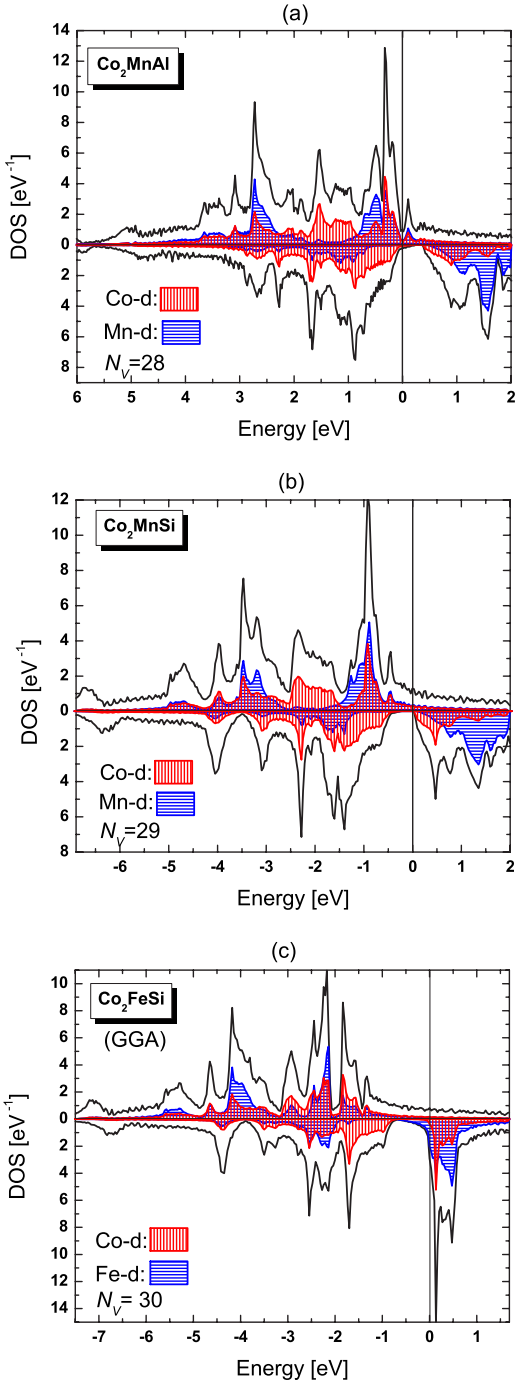

FIG. 5. (Color online) Spin-resolved density of states (DOS) of (a) Co_2MnAl, (b) Co_2MnSi, and (c) Co_2FeSi with 28, 29, and 30 valence electrons, respectively.

rectly, instead they place the Fermi energy above the gap and give a magnetic moment of at most $5.4\mu_B$ [see Fig. 5(c)]. Effects of electron-electron correlation are so important here that the LSDA+U needs to be employed to achieve agreement with the measured data.[4,8] A glance at the calculated DOS of Wurmehl *et al.*[8] shows that E_F is now at the lower portion of the gap, which will reduce the exchange average compared with the LSDA and GGA calculations for which Fig. 5(c) shows the gap to be below E_F. Therefore, it is not surprising that the calculated Curie temperature of 1185 K is that close to the measured value of 1100 K in spite of the larger prefactor expected in the LSDA+U, for which, unfortunately, we cannot yet carry through the detailed calculations necessary for the Curie temperature.

IV. SUMMARY

The Curie temperatures for a set of Co_2-based Heusler compounds have been determined *ab initio* from the ground-state band structure obtained with the local-density functional approximation and/or the generalized gradient approximation. For this purpose, the low-lying excited states were modeled by means of spin spirals characterized by various wave vectors $\mathbf{q}$ that determine the relevant exchange energies as a function of $\mathbf{q}$; these are needed to evaluate the spherical approximation for the Curie temperature given in Eq. (2). The results agree well to very well with experiments and allow us to relate the observed trends to the electronic structure and understand them qualitatively in terms of properties of the density of states. Furthermore, the kind of accuracy achieved will enable predictions to be made for those magnetic compounds for which the Curie temperature has yet to be measured.

ACKNOWLEDGMENT

The authors gratefully acknowledge the financial support by the Deutsche Forschungsgemeinschaft in research unit FG 559.

APPENDIX

The total energy is obtained as a function of the spin-spiral $\mathbf{q}$ vector in eight BZ scans with the following choice of the variables: one scan for $\theta=20°$ and $\varphi=0$ for all atoms, labeled $\Delta E_0(\mathbf{q})$, and another one for $\theta=0$ for atom X and $\theta=20°$ as well as $\varphi=0$ for all atoms, labeled $\Delta E_{00}(\mathbf{q})$. Four more scans, labeled $\Delta E_i(\mathbf{q})$, $i=1-4$, are done with $\varphi_\tau-\varphi_{\tau'}=\mathbf{q}'\cdot(\boldsymbol{\tau}-\boldsymbol{\tau}')$ choosing $\mathbf{q}'=\mathbf{q}+\mathbf{K}_i$ with $\mathbf{K}_1=0$ and $\mathbf{K}_2$ to $\mathbf{K}_4$ being the reciprocal lattice vectors (0,2,0), (1,1,−1), and (1,1,1) in units of $2\pi/a$. Finally, ΔE_5 and ΔE_6 are obtained with $\theta=0$ for atom X and $\theta=20°$ for the other atoms using $\varphi_\tau-\varphi_{\tau'}=\mathbf{q}'\cdot(\boldsymbol{\tau}-\boldsymbol{\tau}')$ with $\mathbf{K}_5=0$ and $\mathbf{K}_6=(1,1,1)$. One scan consists of 60 spiral $\mathbf{q}$ vectors chosen in the irreducible part of the BZ such that the integrals (sums) in Eq. (2) are obtained reliably.

If we define

$$S_a(\mathbf{q}) = \frac{1}{4}\sum_{i=1}^{4} \Delta E_i(\mathbf{q})$$

and

$$S_b(\mathbf{q}) = \frac{1}{2}\sum_{i=5}^{6} \Delta E_i(\mathbf{q})$$

together with

$$f_1 = 4M_1M_2(1-\cos\theta)$$

and

$$f_2 = f_1\cos\theta,$$

then one derives

$$j_{23}(\mathbf{q}) = [\Delta E_{00}(\mathbf{q}) - S_b(\mathbf{q})]/2M_2^2\sin^2\theta$$

and

$$j_{12}(\mathbf{q}) = [\Delta E_0(\mathbf{q}) + S_b(\mathbf{q}) - S_a(\mathbf{q}) - \Delta E_{00}(\mathbf{q})]/4M_1M_2\sin^2\theta$$

as well as

$$j_{11}(\mathbf{q}) = j_{11}(0) + [S_a(\mathbf{q}) - S_b(\mathbf{q}) + j_{12}(0)f_2]/M_1^2\sin^2\theta$$

and

$$j_{22}(\mathbf{q}) = j_{22}(0) + j_{23}(0) + [S_b(\mathbf{q}) + j_{12}(0)f_1]/M_2^2\sin^2\theta.$$

A sum rule for the constants $j_{11}(0)$ and $j_{22}(0)$ allows one to adjust these such that the lowest branch of eigenvalues is zero for $\mathbf{q}=0$ (Goldstone mode). The three branches are given for each wave vector $\mathbf{q}$ by the eigenvalues $j_{n=1}(\mathbf{q}) = j_{22}(\mathbf{q}) - j_{23}(\mathbf{q})$ and

$$j_{n=2,3} = (j_{11}+j_{22}+j_{23})/2 \pm \sqrt{2j_{12}^2 + (j_{11}-j_{22}-j_{23})^2/4},$$

where, for simplicity in writing, the $\mathbf{q}$ dependence of the exchange functions is implied. A special case of this algorithm was given in Ref. 17.

*jkubler@fkp.tu-darmstadt.de

[1] F. Heusler, Verh. Dtsch. Phys. Ges. **5**, 559 (1903).
[2] J. Kübler, A. R. Williams, and C. B. Sommers, Phys. Rev. B **28**, 1745 (1983).
[3] I. Galanakis, P. H. Dederichs, and N. Papanikolaou, Phys. Rev. B **66**, 174429 (2002).
[4] G. H. Fecher, H. C. Kandpal, S. Wurmehl, C. Felser, and G. Schönhense, J. Appl. Phys. **99**, 08J106 (2006).
[5] Y. Miura, K. Nagao, and M. Shirai, Phys. Rev. B **69**, 144413 (2004).
[6] T. Block, C. Felser, G. Jakob, J. Ensling, B. Mühling, P. Gütlich, and R. J. Cava, J. Solid State Chem. **176**, 646 (2003).
[7] H. C. Kandpal, G. H. Fecher, and C. Felser, J. Phys. D **40**, 1507 (2007).
[8] S. Wurmehl, G. H. Fecher, H. C. Kandpal, V. Ksenofontov, C. Felser, H.-J. Lin, and J. Morais, Phys. Rev. B **72**, 184434 (2005).
[9] S. Picozzi, A. Continenza, and A. J. Freeman, Phys. Rev. B **69**, 094423 (2004).
[10] T. Marukame, T. Ishikawa, S. Hakamata, K. Matsuda, T. Uemura, and M. Yamamoto, Appl. Phys. Lett. **90**, 012508 (2007).
[11] N. Tezuka, N. Ikeda, S. Sugimoto, and K. Inomata, Appl. Phys. Lett. **89**, 252508 (2006).
[12] Y. Sakuraba, M. Hattori, M. Oogane, Y. Ando, H. Kato, A. Sakuma, T. Miyazaki, and H. Kubota, Appl. Phys. Lett. **88**, 192508 (2007).
[13] W. Kohn and L. J. Sham, Phys. Rev. **140**, A1133 (1965).
[14] J. Kübler, *Theory of Itinerant Electron Magnetism* (Clarendon, Oxford, 2000).
[15] J. B. Staunton, Rep. Prog. Phys. **57**, 1289 (1994).
[16] T. Moriya, *Spin Fluctuations in Itinerant Electron Magnetism* (Springer-Verlag, Berlin, 1985).
[17] J. Kübler, J. Phys.: Condens. Matter **18**, 9795 (2006).
[18] J. P. Perdew, K. Burke, and M. Ernzerhof, Phys. Rev. Lett. **77**, 3865 (1996).
[19] C. Herring, in *Magnetism IV*, edited by G. Rado and H. Suhl (Academic, New York, 1966).
[20] L. M. Sandratskii, J. Phys. F: Met. Phys. **16**, L43 (1986).
[21] L. M. Sandratskii, Adv. Phys. **47**, 91 (1998).
[22] Q. Niu and L. Kleinman, Phys. Rev. Lett. **80**, 2205 (1998).
[23] Q. Niu, X. Wang, L. Kleinman, W.-M. Liu, D. M. C. Nicholson, and G. M. Stocks, Phys. Rev. Lett. **83**, 207 (1999).
[24] V. Heine, in *Solid State Physics*, edited by H. Ehrenreich, F. Seitz, and P. Turnbull (Academic, New York, 1980), Vol. 35.
[25] A. R. Mackintosh and O. K. Andersen, in *Electrons at the Fermi Surface*, edited by M. Springford (Cambridge University Press,

Cambridge, 1980).
[26] K. H. J. Buschow and P. G. van Engen, J. Magn. Magn. Mater. **25**, 90 (1981).
[27] P. G. van Engen, K. H. J. Buschow, and M. Erman, J. Magn. Magn. Mater. **30**, 374 (1983).
[28] P. J. Webster, J. Phys. Chem. Solids **32**, 1221 (1971).
[29] K. R. A. Ziebeck and K.-U. Neumann, in *Alloys and Compounds of d-Elements with Main Group Elements*, edited by H. P. J. Wijn, Landolt-Börnstein, New Series Group III, Vol. 32, Pt. C (Springer-Verlag, Heidelberg, 2001), Pt. 2, pp. 64–314.
[30] R. Y. Umetsu, K. Kobayashi, A. Fujita, K. Oikawa, R. Kainuma, K. Ishida, N. Endo, K. Fukamichi, and A. Sakuma, Phys. Rev. B **72**, 214412 (2005).
[31] S. Wurmehl, G. H. Fecher, H. C. Kandpal, V. Ksenofontov, C. Felser, and H.-J. Lin, Appl. Phys. Lett. **88**, 032503 (2006).
[32] S. Wurmehl, G. H. Fecher, V. Ksenofontov, F. Casper, U. Stumm, C. Felser, H.-J. Lin, and Y. Hwu, J. Appl. Phys. **99**, 08J103 (2005).
[33] A. R. Williams, J. Kübler, and C. D. Gelatt, Phys. Rev. B **19**, 6094 (1979).
[34] U. von Barth and L. Hedin, J. Phys. C **5**, 1629 (1972).
[35] K. Knöpfle, L. M. Sandratskii, and J. Kübler, Phys. Rev. B **62**, 5564 (2000).
[36] S. Wurmehl, G. H. Fecher, K. Kroth, F. Kronast, H. Dürr, Y. Takeda, Y. Saitoh, K. Kobayashi, H.-J. Lin, G. Schönhense, and C. Felser, J. Phys. D **39**, 803 (2006).
[37] M. Ležaić, P. Mavropoulos, J. Enkovaara, G. Bihlmayer, and S. Blügel, Phys. Rev. Lett. **97**, 026404 (2006).